Proceedings of the 2019 Hypervelocity Impact Symposium
HVIS2019
April 14-19, 2019, Destin, FL, USA
HVIS2019-004

Calculation of jet characteristics from hydrocode analysis

Justin C. Sweitzer[a]*, Nicholas Peterson[b], and Scott Hill[a]

[a]*Practical Energetics Research, Inc. Huntsville, AL, 35802*
[b]*US Army CCDC-AvMC, Redstone Arsenal, AL 35878*

Abstract

The penetration performance of a shaped charge jet is affected strongly by factors such as straightness, stretch rate, and breakup time. Straightness is related to manufacturing tolerances, assembly techniques, and system integration features. Stretch rate and breakup time are controllable features of charge design. A higher stretch rate is desirable for short standoff performance. The stretch rate is easily altered by a change of explosive or modification of the angle with which the detonation wave sweeps the liner surface, however, an increased stretch rate generally results in a decreased breakup time. Many of the recent gains in shaped charge performance have been made possible by increasing the effective breakup time of the jet.

Several models exist for calculating breakup time. They include analytic models, such as Chou & Carleone's dimensionless strain rate model, and empirical or semi-empirical models such as Walsh's theory and those proposed by Pearson, et al. These models can be applied to raw hydrocode calculation data and used to determine a Jet Characterization (JC) file. The JC file can then be used to perform further calculations, such as Penetration Versus Stand Off (PVSO) curves.

This paper details adaptation of the Chou & Carleone model for predicting breakup time using hydrocode data. The hydrocode is used to determine the physical parameters of the jet which are then extrapolated back to a virtual origin for breakup time calculation. This results in a model that is design independent, relying on hydrocode determination of jet variables. The model implementation will be discussed, and comparisons of predicted jet characteristics will be made to test data for several charge geometries.
.

Keywords: Shaped charges, Breakup, Fragmentation

1. Introduction

Many empirical relationships for the breakup time of a shaped charge jet have been derived, including those put forward by Hirsch[1–4] , Pfeffer[5], Haugstad[6], and Haugstad & Dullum[7]. Hirsch[1] related the breakup time to a simple ratio of jet diameter to plastic wave velocity. This model provides reasonable estimates of breakup time within a very narrow range of charge geometries, but lacks a dependence on strain rate.[8]

Pfeffer[5] performed numeric simulation to empirically arrive at a relationship with inverse dependence on strain rate and a direct relationship with the ratio of jet radius to shock velocity in the jet material. This model neglects the jet strength of Hirsch's model (in the form of plastic wave velocity), and thus also finds limited application. Haugstad[6] and Haugstad & Dullum[7]

* Corresponding author. Tel.: +1-256-867-1222.
E-mail address: justin.sweitzer@per-hq.com.

formulate relationships within a continuum mechanics framework that depend on a hydrodynamic description of the jet strength, with an initial yield stress supplemented by an artificial viscosity term.

Walsh[9] developed a dimensionless 'instability parameter', which includes yield strength, density, initial stretch rate, and jet radius. Breakup time is correlated to this parameter through a critical value, which is material dependent. Walsh's results have been further developed in recent history. In Baker, et al[10], correlations are developed building off of a previous study[11] focused on molybdenum liners, to describe average particle lengths, number of particles, and breakup times. Their metric of choice is the cubic root of the derivative of accumulated mass with respect to jet velocity, and they show this parameter to be closely related to the Walsh parameter.

Chou & Carleone[12] developed an analytic relationship[13,14] between a dimensionless breakup time and dimensionless initial strain rate. The formula is expressed

$$\bar{t}_b = 3.75 - 0.125\bar{\eta}_0 + \frac{1}{\bar{\eta}_0} \qquad 1$$

The dimensionless breakup time is the ratio of breakup time t_b multiplied by plastic wave velocity, $C_p = \sqrt{Y/\rho}$, where Y and ρ are yield strength and density, and initial jet radius r_0, or $\bar{t}_b = t_b C_p / r_0$. The dimensionless strain rate is $\bar{\eta}_0 = \dot{\varepsilon}_0 r_0 / C_p$, where $\dot{\varepsilon}_0$ is the initial strain rate. This model has also been shown to closely approximate breakup time across a wide range of charge geometries and liner materials[8]. They provide correlations including an empirical correction factor[15] in later works, which is reviewed by Walters & Summers[8,16].

Hennequin[17] proposed a model for a conical copper shaped charge introducing a 'fragment shape index' which is determined experimentally. The model represents elements of Hirsch's and Chou & Carleone's developments with correction terms based on the average shape of jet particles. The calculated results represent a marginal improvement over Chou & Carleone, while requiring empirical characterization of the shape index. The simplicity and accuracy of the Chou and Carleone model, and the wide availability of the required mechanical data for liner materials lead to the selection of this model for integration with hydrocode calculation in this work.

2. Hydrocode Integration

Shaped charge design is largely approached today through iterative simulation/test cycles. Hydrocode analysis is used to identify trends in desired performance traits and design candidates are prototyped and tested to provide validation and improve model fidelity. One of the challenges of this design approach is the calculation of jet breakup times. Hydrocode simulations are capable of closely predicting jet characteristics such as velocity and mass gradients, but diverge from experiment when estimating material failure. Finite element simulations introduce artificial sources of jet instability through mesh resolution, and failure models tend to produce inaccurate estimates of breakup at high strain rates.[18]

A combined approach leveraging the hydrocode predictions of jet characteristics with the Chou & Carleone breakup model can easily be implemented, allowing breakup time to be treated as a design variable. In the current work, the ALE3D hydrocode[19] is used to simulate the jet formation, and the jet characteristics are extracted through the Visualization Toolkit (VisIt)[20,21]. An external Python code is then used to calculate the breakup times. The output of the Python code is in the format used by Dyna East's WASP program, which can be used to predict penetration performance.

The Chou & Carleone model predicts breakup time as a function of local strain rate, and does not provide particle-by-particle estimates of length. In order to divide the jet into discrete particles, a stochastic natural fragmentation model[22–24] is used to determine the average particle length. This model was derived for the case of a one-dimensional rod stretching uniformly in tension. The mean length is

$$\bar{l} = \phi\sqrt{\frac{\pi}{2}}l_1 + (1-\phi)1.48l_2, \qquad \phi = \mathrm{erf}\left(\sqrt[4]{\frac{Y\dot{\varepsilon}r_0^3}{\rho c^3}}\right) \qquad 2$$

In the above equation, c is the material sound speed, and l_1, l_2 are length scales for brittle and ductile fracture models. The parameter ϕ is an estimate of dynamic ductility, and is the probability of a brittle-like fracture completing before plastic deformation can relieve stress in a rapidly propagating crack. The length scales are

$$l_1 = \sqrt[4]{\frac{\sigma^2}{\rho}\frac{Yc}{r_0\dot{\varepsilon}^3}}, \qquad l_2 = \sqrt[3]{\frac{3\sigma}{2}\frac{Y}{\rho\dot{\varepsilon}^2}}, \qquad \sigma = 4.5\sqrt{\frac{2Y}{\rho\dot{\varepsilon}^2\gamma^3}}$$

The γ in the above set of equations is the Mott physics-based[25] distribution parameter, and can be estimated from the Johnson-Cook constitutive model[26] as

$$\gamma \sim \frac{160Bn\varepsilon^{n-1}}{A + B\varepsilon^n}$$

More complete details of the model derivation can be found in the references[22–24].

3. Hydrocode Integration

The first step of this approach is a 2D, axisymmetric hydrocode simulation. Where available, the Johnson-Cook constitutive model is preferred for the liner material, as the Mott γ is calculated from the parameters. The Johnson-Cook parameters are held constant, and not applied as statistical distribution functions. The validation studies reported in latter sections of this paper were performed with a mesh density of 3 zones/mm. No mesh resolution sensitivity analysis has been performed at this point.

The hydrocode model is allowed to run until the jet has completely formed, and radial components of velocity have approached zero. Data is extracted from the simulation at this point, and post-processing begins. In order to ensure that the calculations are less dependent on the time from which the jet characterization data is extracted, the jet is moved to a common reference frame. Initially, the virtual origin was used for this purpose, but for waveshaped and non-conical charge geometries this approximation does not hold well. Instead, the reference frame was chosen as the point where the jet tip is two charge diameters from the initial liner face. The choice of reference frame is somewhat arbitrary, in that it was chosen based on a very limited-scope sensitivity study using a single warhead geometry. The jet is moved to this location by allowing the velocity gradient to determine the new coordinates and conserving mass by increasing jet radius, treating each differential segment of jet as a cylinder. This choice of reference frame is somewhat in conflict with the Chou-Carleone assumptions, which are based around the initial state immediately after collapse of the jet element.

Again, the virtual origin would be the ideal location to satisfy these assumptions, but the wide variance of the error in the virtual origin approximation for non-conical liners prohibits its use here. An additional challenge with this approach is that the jet is stretching in free flight, converting some of the kinetic energy into internal energy. Translating the jet in space and conserving mass and velocity, as has been done here, therefore does not conserve energy. Calculation accuracy and timestep independence would be improved by a more thorough description of jet kinematics, such as presented in Babkin, et al[27,28].

With the jet in the common frame of reference, Eq. 2 is used to determine the average particle length, and the number of particles is calculated by dividing the total length by particle length. The jet is segmented into the total number of particles using the velocity gradient as the binning factor. This produces shorter particles toward the front of the jet, where the strain rate is higher, and longer particles toward the back where the strain rate is lower. The breakup time is then calculated using Eq. 1 for each individual particle. Because the particle size calculation is performed assuming fracture occurs around the reference frame, the results reflect a material with an average breakup length of two charge diameters. Performing the breakup time calculation provides an estimate of actual strain-to-failure. The final step in the process, then, is to stretch the particle out to the calculated breakup time.

4. Results

The first comparison made here is to data collected for the Viper warhead[29]. Viper is a 65 mm diameter, 44° conical copper shaped charge. Figure 1 below shows the calculated accumulated mass versus velocity plots alongside the experimental data. The calculations show a slower tip speed than the experimental results, but generally follow along with the experimental data. The experimental data shows 79 particles down to an axial velocity of 2 km/s. By comparison, the calculations result in 75 particles at roughly the same velocity. Scaled cumulative jet lengths are compared in Figure 2a, which indicates that the calculated particle lengths are very close to the experimental particle lengths. Divergence occurs at the tip and tail in the same locations as the cumulative mass profiles diverge.

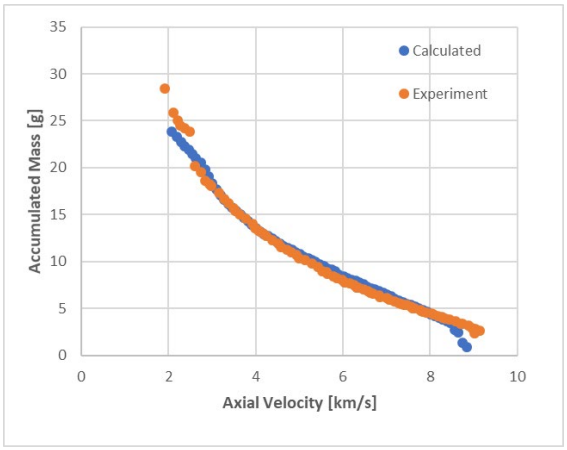

Figure 1. Accumulated mass versus velocity for Viper charge

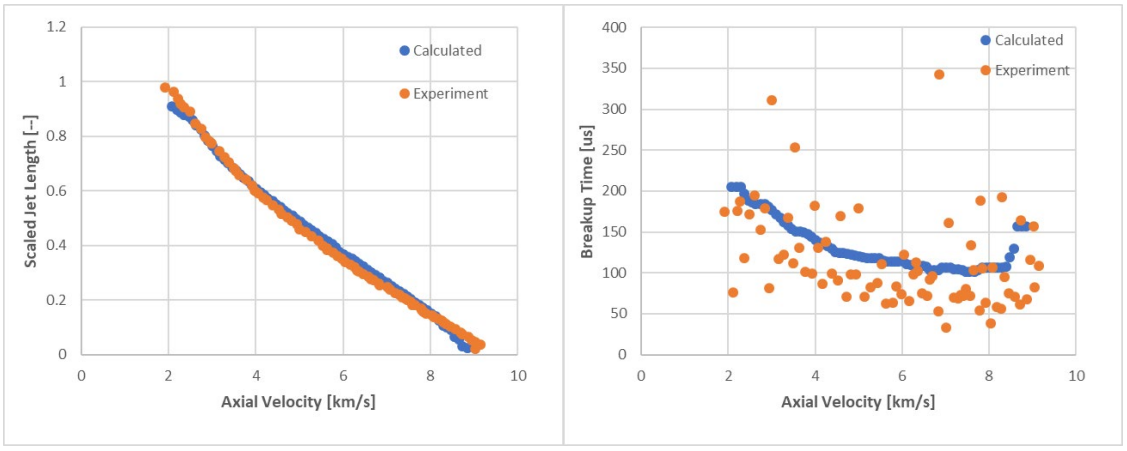

Figure 2. Scaled accumulated length versus velocity (a) and breakup time (b) for Viper charge

Figure 2b shows the breakup time comparison. The average calculated breakup time is 132 us, compared to the experimental result of 125 us. The experimental breakup time is estimated by the distance from the tail of the ith particle to the tip of the i+1th particle divided by the velocity difference. Across the range of axial velocities, the calculated breakup time is near the top of the range of observed values.

A second comparison is made for a 60 mm, waveshaped molybdenum cone[11]. This charge is designed to produce a fast, low mass jet. The Steinberg-Guinan strength model was used for molybdenum, as opposed to the Johnson-Cook constitutive equation for copper. The accumulated mass profile in Figure 3 shows more divergence between the hydrocode and

experimental results. This may be a result of constitutive model inaccuracies for the Steinberg-Guinan model employed for molybdenum in ALE3D. It could also arise from tolerance stackups in the manufacturing process. The calculated values of jet length in Figure 4a are accordingly shorter than the experimental values, but the calculated breakup times in Figure 4b are in line with the observed values.

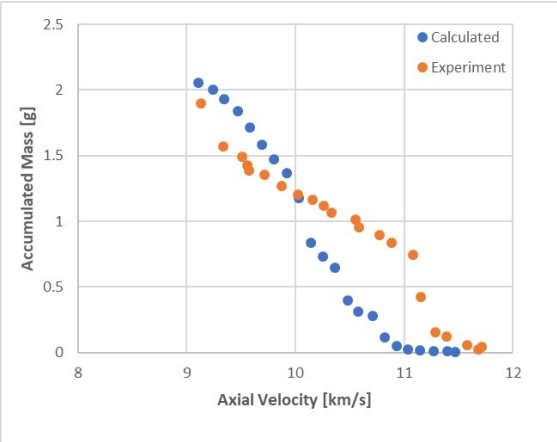

Figure 3. Accumulated mass versus velocity for 60 mm Waveshaped Mo Cone

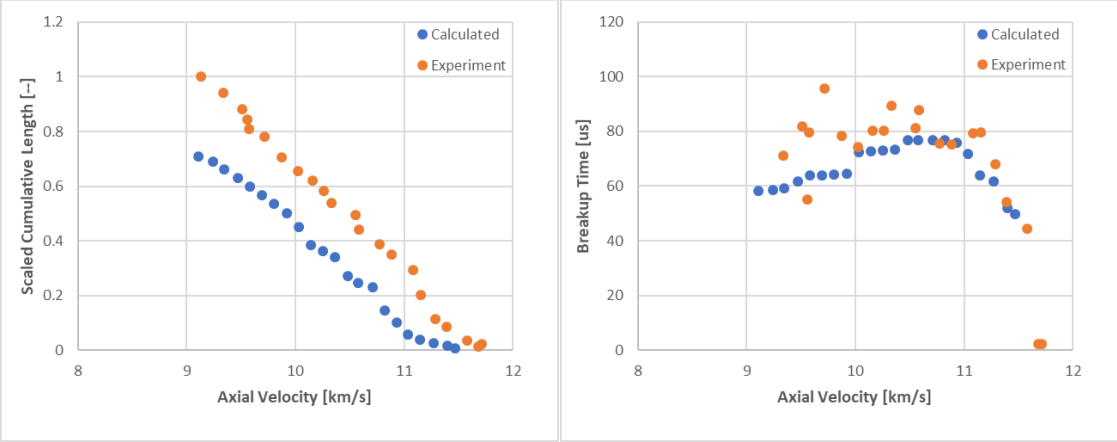

Figure 4. Scaled acc. length (a) and breakup time (b) vs velocity for 60 mm Waveshaped Mo Cone

A final comparison is made for NHN1-2, which is a 165 mm, waveshaped copper liner with experimental data from Pham, et al[30]. The accumulated mass profile in Fig 5 shows good agreement between the hydrocode and experimental data, with some minor overprediction of tip speed. There is also small divergence at the tail, where the experimental data shows that the last two particles are comparatively large. The scaled accumulated length profile depicted in figure 6a also indicates good agreement with the experimental data. The calculated breakup times in Fig. 6b show reasonable agreement with the experimental data, which appears to have been linearized in the source report[30]. The calculated average breakup time is 334 us in comparison to the experimental 352 us.

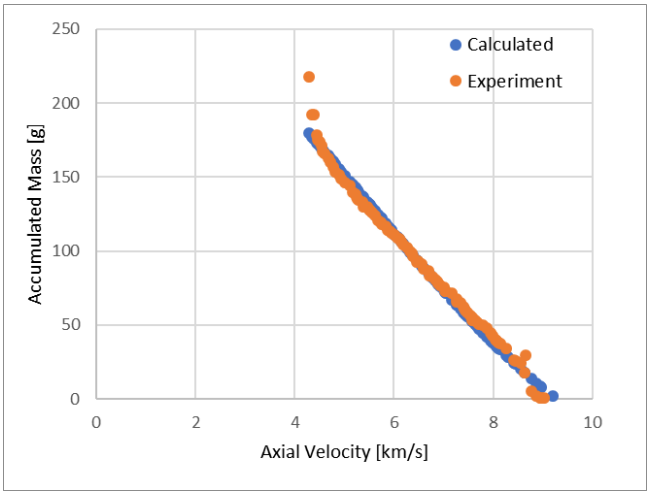

Figure 5. Accumulated mass versus velocity for NHN1-2

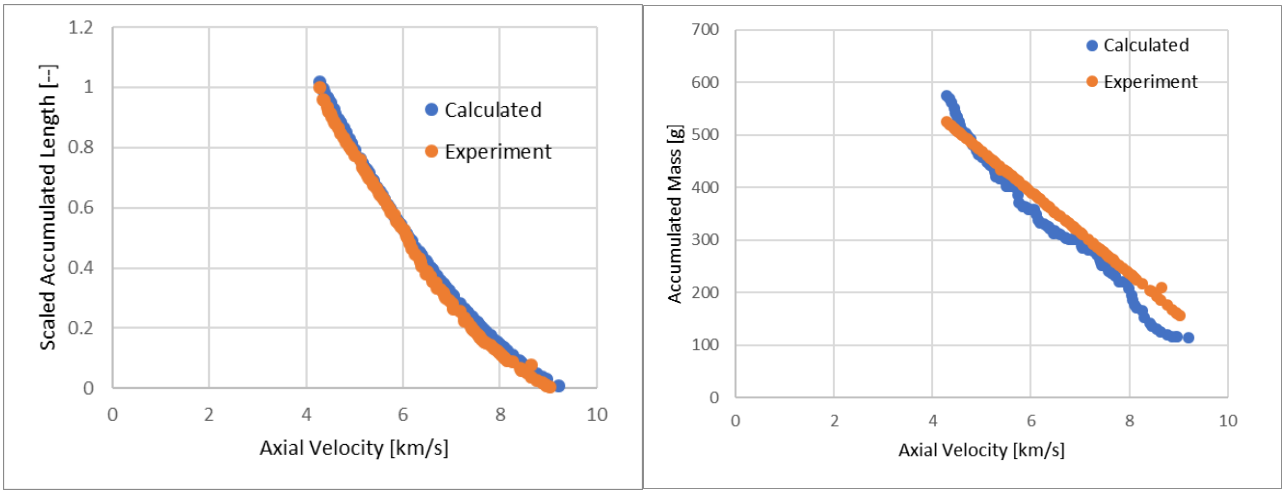

Figure 6. Scaled acc. length (a) and breakup time (b) vs velocity for NHN1-2.

A summary of average characteristics observed versus calculated appears in Table 1.

Table 1. Summarized comparisons.

	Tip Speed		Scaled Length		Average Breakup		Number of Particles	
	km/s		--		us		--	
	Observed	Calculated	Observed	Calculated	Observed	Calculated	Observed	Calculated
Viper	9.02	8.84	1	0.91	125	132.4	79	75
Mo Cone	11.7	11.5	1	0.71	60.1	66.7	22	23
NHN1-2	9.03	9.2	1	1.07	352	334	93	97

5. Conclusions

The simulation approach tends to produce effective estimates of breakup time for a straight wall, conical liner and waveshaped

molybdenum and copper liners. More extensive validation of the model predictions will be undertaken, including calculations for additional liner materials and charge geometries (where experimental data is available). Additionally, more complete descriptions of jet kinematics[27,28] will be implemented in the post-processing code for translating the jet between formation, reference, and final breakup locations. This is expected to further reduce the dependence on the timestep and improve the accuracy of the calculations.

Currently the Chou-Carleone model is implemented in the post-processing code as the breakup time relationship because of the simplicity and availability of input parameters. Additional models will be implemented alongside this option and evaluated for consistency and accuracy of results. The ability to perform shaped charge simulation with extensive jet characterization as the output is becoming more necessary in modern iterative design processes.

In addition, more formal sensitivity analyses should be performed regarding the choice of reference frame and mesh density in the hydrocode calculation.

6. References

1. Hirsch, E. A Formula for the Shaped Charge Jet Breakup-Time. *Propellants, Explos. Pyrotech.* **4**, 89–94 (1979).
2. Hirsch, E. A Model Explaining the Rule for Calculating the Break-up Time of Homogeneous Ductile Metals. *Propellants Explos.* **6**, 11–14 (1981).
3. Hirsch, E. The Effect of the Liner Metallurgical State on the shaped charge jet break-up time. *Propellants, Explos. Pyrotech.* **15**, 166–176 (1990).
4. Hirsch, E. Scaling of the shaped charge jet break-up time. *Propellants, Explos. Pyrotech.* **31**, 230–233 (2006).
5. Pfeffer, G. Détermination par simulations numériques de l'état et des lois de fragmentation des jets de charges creuses. in *Proc. 5th Int. Symp. on Ballistics.* (1980).
6. Haugstad, B. On the Break-Up of Shaped Charge Jets. *Propellants Explos. Pyrotech.* **8**, 119–120 (1983).
7. Haugstad, B. S. & Dullum, O. S. Optimization of shaped charges. *J. Appl. Phys.* **55**, 100–106 (1984).
8. Walters, W. P. & Summers, R. L. A Review of Jet Breakup Time Models. *Propellants Explos. Pyrotech.* **18**, 241–246 (1993).
9. Walsh, J. M. Plastic instability and particulation in stretching metal jets. *J. Appl. Phys.* **56**, 1997–2006 (1984).
10. Baker, E. L., Pham, J. & Vuong, T. *An Empirical Shaped Charge Jet Breakup Model*. (2014).
11. Baker, E. L., Daniels, A., Pham, J., Vuong, T. & Defisher, S. JET BREAK-UP CHARACTERIZATION OF MOLYBDENUM SHAPED CHARGE LINERS. in *2003 Society for Experimental Mechanics Conference* (2003).
12. Chou, P. C. & Carleone, J. The stability of shaped-charge jets. *J. Appl. Phys.* **48**, 4187–4195 (1977).
13. Chou, P. C. & Flis, W. J. Recent Developments in Shaped Charge Technology. *Propellants, Explos. Pyrotech.* **11**, 99–114 (1986).
14. Chou, P. C., Tanzio, C. A., Carleone, J. & Cicarelli, R. D. *SHAPED CHARGE JET BREAKUP STUDIES USING RADIOGRAPH MEASUREMENT AND SURFACE INSTABILITY CALCULATIONS*. (1977). doi:10.1109/CSMR.2012.24
15. Chou, P. C., Grudza, M., Liu, Y. F. & Ritzman, Z. Shaped-Charge Jet Break-Up Formula with Metal Anisotropy. in *Proceedings of the 13th International Symposium on Ballistics (Vol 2)* (1992).
16. Walters, W. P. & Summers, R. L. The Particulation of a Shaped Charge Jet for Face-Centered-Cubic Liner Materials. *Arl-Tr-114* 60 (1993).
17. Hennequin, E. Modelling of the shaped charge jet break-up. *Propellants, Explos. Pyrotech.* **21**, 181–185 (1996).
18. Petit, J., Jeanclaude, V. & Fressengeas, C. Breakup of Copper shaped-charge jets: Experiment, numerical simulations, and analytical modeling. *J. Appl. Phys.* **98**, 123521 (2005).
19. Nichols (ed), A. *User's Manual for ALE3D: An Arbitrary Lagrange/Eulerian 3D Code System*. (2007).
20. Childs, H. VisIt: An End-User Tool for Visualizing and Analyzing Very Large Data. (2013).
21. *VisIt Python Interface Manual*. (2013).
22. Sweitzer, J. C. & Banish, R. M. A closed form, energy-based theory of dynamic fragmentation. *J. Appl. Phys.* **123**, 075901 (2018).
23. Sweitzer, J. C., Hill, S. D. & Banish, R. M. Energy based distribution for naturally fragmenting warheads. in *California: Joint Classified Bombs/Warheads & Ballis-tics Symposium Monterey* 1–4 (2016).

24. Sweitzer, J. C. Material Sections and Natural Fragmentation Size Distributions in Heterogenous Shells: A Dissertation. (University of Alabama in Huntsville, 2016).
25. Mott, N. F. Fragmentation of Shell Cases. *Proc. R. Soc. A Math. Phys. Eng. Sci.* **189**, 300–308 (1947).
26. Johnson, G. R. & Cook, W. H. A constitutive model and data for metals subjected to large strains, high strain rates and high temperatures. *7th International Symposium on Ballistics* 541–547 (1983). doi:10.1038/nrm3209
27. Babkin, A. V., Ladov, S. V., Marinin, V. M. & Fedorov, S. V. Characteristics of inertially stretching shaped-charge jets in free flight. *J. Appl. Mech. Tech. Phys.* **38**, 171–176 (1997).
28. Babkin, A. V, Ladov, S. V, Marinin, V. M. & Fedorov, S. V. Regularities of the stretching and plastic failure of metal shaped- charge jets. *J. Appl. Mech. Tech. Phys.* **40**, 571–580 (1999).
29. Fermen-Coker, M. *A 2-D Axisymmetric Model of a Stretching Jet in ALEGRA*. (2004).
30. Pham, J. D., Baker, E. L. & Defisher, S. *SHAPED CHARGE JET FLASH RADIOGRAPH DIGITIZATION*. (2005).